



Enhancement of the finite-frequency superfluid response in the pseudogap regime of strongly disordered superconducting films

Mintu Mondal¹, Anand Kamlapure¹, Somesh Chandra Ganguli¹, John Jesudasan¹, Vivas Bagwe¹, Lara Benfatto² & Pratap Raychaudhuri¹

¹Tata Institute of Fundamental Research, Homi Bhabha Road, Colaba, Mumbai 400005, India, ²ISC-CNR and Department of Physics, Sapienza University of Rome, Piazzale Aldo Moro 5, 00185, Rome, Italy.

Received
18 December 2012

Accepted
18 February 2013

Published
28 February 2013

Correspondence and
requests for materials
should be addressed to
P.R. (pratap@tifr.res.
in)

The persistence of a soft gap in the density of states above the superconducting transition temperature T_c , the pseudogap, has long been thought to be a hallmark of unconventional high-temperature superconductors. However, in the last few years this paradigm has been strongly revised by increasing experimental evidence for the emergence of a pseudogap state in strongly-disordered conventional superconductors. Nonetheless, the nature of this state, probed primarily through scanning tunneling spectroscopy (STS) measurements, remains partly elusive. Here we show that the dynamic response above T_c obtained from the complex ac conductivity, is highly modified in the pseudogap regime of strongly disordered NbN films. Below the pseudogap temperature, T^* , the superfluid stiffness acquires a strong frequency dependence associated with a marked slowing down of critical fluctuations. When translated into the length-scale of fluctuations, our results suggest a scenario of thermal phase fluctuations between superconducting domains in a strongly disordered s-wave superconductor.

At the microscopic level, the superconducting (SC) state is characterized by two remarkable properties: (i) the pairing of electrons in bound states, i.e. Cooper pairs, leading to a gap Δ in the electronic excitation spectrum and (ii) the formation of a macroscopic phase coherent state of the Cooper pairs, responsible for the SC behavior. Based on the conventional Bardeen-Cooper-Schrieffer theory¹, one expects the SC transition to happen at the temperature where Δ goes to zero², since the energy cost of twisting the phase of the condensate, i.e. the superfluid stiffness J , is usually much larger than Δ . However, this central paradigm has been questioned within the context of underdoped high-temperature superconductors, where the pairing scale Δ , associated to the pseudogap (PG) state, is much larger than J , which gets reduced by the proximity to the Mott insulator³. More recently a series of experiments on strongly disordered s-wave superconductors^{4–6} (TiN, InO_x and NbN) outlined a scenario, that bears some similarities with the case of high-temperature superconductors. Indeed, on the one hand it has been shown that a soft gap in the electronic excitation spectrum continues to persist in the tunneling density of states (t-DOS) up to a temperature T^* , well above T_c . On the other hand disorder scattering reduces J , thereby rendering the system susceptible to phase fluctuations³. In addition, STS measurements revealed that at strong disorder the superconducting state becomes inhomogeneous, segregating into domains where the SC order parameter is large and regions where the order parameter is completely suppressed^{6–8}. From the theoretical standpoint it is now understood that disorder contributes to maintain the pairing scale finite at strong disorder, while phase fluctuations can drive the transition^{9–11}. At the same time it has been suggested that strong disorder can induce a direct superconductor-insulator transition (SIT) by localization of Cooper pairs¹². In such scenario several additional predictions have been made^{12,13} concerning the emergence of physical effects remnant of a glassy behavior, that can be evidenced for example by the statistical analysis of the inhomogeneous order-parameter distribution observed by STS far below⁸ T_c . However, a clear picture of the relation between all these effects in the pseudogap (PG) state is still lacking, due to the inability of STS to probe the superfluid response of the system.

In this article, we address this problem through measurement of the ac complex conductivity, $\sigma(\omega) = \sigma'(\omega) + i\sigma''(\omega)$, on NbN thin films with different levels of disorder using a broadband Corbino



microwave spectrometer^{14–16} operating in the frequency range, $f \equiv \frac{\omega}{2\pi} = 0.1 - 20$ GHz. The advantage of this technique is that it is sensitive to superconducting correlations over finite time scales. Thus, it allows one to probe directly the remnant superfluid response of the system above T_c , that is the crucial quantity to look at in order to outline the nature of the PG state. In addition, the length scale of electron diffusion at microwave frequency is of the order of the nanometers, i.e. the same order of the inhomogeneity probed by STS. We then expect that this technique can also give us indirectly a picture of the spatial variation of the SC properties in the PG state, whose relevance below T_c has been well established by STS measurements^{6–8}. In the superconducting state, where phase coherence extends over all length and time scales, the superfluid density (n_s) and hence J can be determined from $\sigma''(\omega)$ using the relations^{2,3},

$$\sigma''(\omega) = \frac{n_s e^2}{m\omega} \quad \text{and} \quad J = \frac{\hbar^2 n_s a}{4m}, \quad (1)$$

where e and m are the electronic charge and mass respectively, and a is the length scale associated with phase fluctuations, that is typically of the order of the dirty-limit coherence length, ξ_0 . Above T_c one can define a frequency-dependent stiffness $J \propto \omega \sigma''(\omega)$ which vanishes as $\omega \rightarrow 0$ but survives as long as SC correlations are finite on the time scale set by the inverse frequency. For ordinary Ginzburg-Landau (GL) like SC fluctuations^{17,18}, short-lived Cooper pairs give a finite response over a small temperature and frequency range above T_c due to the fact that the typical frequency scale of Cooper pairs $\omega_0 \sim (T - T_c)/T_c$ becomes soft only near the transition. While this is indeed the case for our less disordered samples, the central observation of this study is that in strongly disordered NbN films, J becomes strongly dependent on the probing frequency below T^* , signaling an unexpected slowing down of the SC fluctuations. The persistence of the high-frequency superfluid response up to T^* supports the scenario where the PG state consists of phase incoherent, slowly fluctuating domains while the superconducting state emerges at T_c when global phase coherence is established between all the domains.

Results

NbN as a model system to study the interplay of superconductivity and disorder. Samples used in this study consist of a set of epitaxial NbN thin films¹⁹ with different levels of disorder grown on single crystalline MgO substrates. The disorder is in the form of Nb vacancies in the NbN crystal lattice which is tuned by controlling the deposition conditions. T_c , defined as the temperature at which dc resistance goes below our measurable limit varies in the range $T_c \approx 15.71 - 3.14$ K. The effective disorder, characterized using the product of the Fermi wave vector, k_F , and electronic mean free path, l , is in the range $k_F l \sim 9.5 - 1.8$. The thickness (t) of all films was ~ 50 nm which is much larger than the dirty limit coherence length²⁰, $\xi_0 \sim 4 - 8$ nm. The phase diagram of disordered NbN established earlier from STS and transport measurements on similar samples²¹ reveal that samples with $T_c < 6$ K show a pronounced PG phase with $T^* \sim 6 - 7$ K.

Complex conductivity as a function of frequency and temperature.

Figure 1(a)–(b) shows the representative data for $\sigma'(\omega)$ and $\sigma''(\omega)$ as a function of frequency at different temperatures for the sample with $T_c \sim 3.14$ K. Consistent with the expected behavior in the superconducting state, at low temperatures $\sigma'(\omega)$ shows a sharp peak as $\omega \rightarrow 0$ whereas $\sigma''(\omega)$ varies as $1/\omega$ (dashed line). Well above T_c , $\sigma'(\omega)$ is flat and featureless and $\sigma''(\omega)$ is within the noise level of our measurement consistent with the behavior in a normal metal at frequencies much smaller than the quasiparticle scattering rate, which is of the order of 10^{16} Hz in our NbN samples²². Figure 2(a)–(d) shows $\sigma'(\omega)-T$, $\sigma''(\omega)-T$ and $J-T$ at different frequencies for four samples with different T_c . All samples display a

dissipative peak in $\sigma'(\omega)$ close to T_c . For low disordered samples $\sigma''(\omega)$ for all frequencies dropped below our measurement limit close to T_c . As shown later the narrow fluctuation regime in these samples is well described by GL Cooper-pairs fluctuations. On the other hand, samples with higher disorder show an extended fluctuation regime where $\sigma''(\omega)$ remains finite up to a temperature well above T_c . We convert $\sigma''(\omega)$ into J (from eqn. 1) using the experimental values of ξ_0 obtained from upper critical field measurements²⁰. For $T \ll T_c$, J is frequency independent, showing that the phase rigidity is established over all time scales. However, for the samples with higher disorder (Fig. 2(c) and 2(d)), J becomes strongly frequency dependent above T_c : While at 0.4 GHz J falls below our experimental threshold, $J \leq 5 * 10^{-4} J(T = T_c)$, very close to T_c , with increase in frequency it acquires a long tail and remains finite well above T_c .

Connection with the pseudogap state observed from STS measurements.

To understand the connection between these observations and the PG state observed in STS measurements²¹, we define $T_m(f)$ as the temperature above which $J(f, T) \leq 5 * 10^{-4} J(f \rightarrow 0, T = T_c)$. The variation of T_m with frequency shows a trend which saturates at high frequencies and can be fitted well with an empirical relation of the form, $(T_m(f) - T_c) = A(1 - e^{-f/f_0})$ (Fig. 3 (a–b)). Using the best fit values of A and f_0 , we determine the limiting value, $T_m^* = T_m(f \rightarrow \infty)$. In Figure 3(c), we plot T_m^* and T_c for several samples along with the variation of T^* and T_c obtained from STS measurements, as a function of $k_F l$. Within the error limits of determining these temperatures, $T^* \approx T_m^*$, showing that the onset of the PG in the t-DOS coincides with the onset of finite J in the high frequency limit. Furthermore, only the samples in the disorder range where a PG state appears, show a large difference between T_c and T_m^* . We therefore attribute the frequency dependence of J to a fundamental property related to the PG state.

Slowing down of critical fluctuations in the pseudogap regime.

Having established the relation between the PG state and the finite high frequency phase stiffness, we now look at the fluctuation region above T_c more closely. On very general grounds, the fluctuation conductivity, $\sigma_{fl}(\omega)$ is predicted²³ to scale at each temperature as $\sigma_{fl}(\omega)/\sigma_{fl}(0) = S(\omega/\omega_0)$, where $\omega_0(T)$ is a characteristic fluctuation frequency. We obtain $\sigma_{fl}(\omega)$ from $\sigma(\omega)$ by subtracting the dc value of the conductivity above T_m^* . Since the phase angle $\phi(\omega) = \tan^{-1}(\sigma''_{fl}(\omega)/\sigma'_{fl}(\omega))$ is the same as the phase angle of S , by scaling $\phi(\omega)$ at each temperature with a different ω_0 one can expect a collapse of all data on a single curve. $|\sigma_{fl}(\omega)|$ would similarly scale when normalized by $\sigma_{fl}(0)$ for the same values of ω_0 at each temperature. Such a scaling works for all the samples in the frequency range 0.4 – 12 GHz as shown in Figure 4(a) and 4(b) for the samples with $T_c \sim 15.71$ K and 3.14 K respectively. We observe a

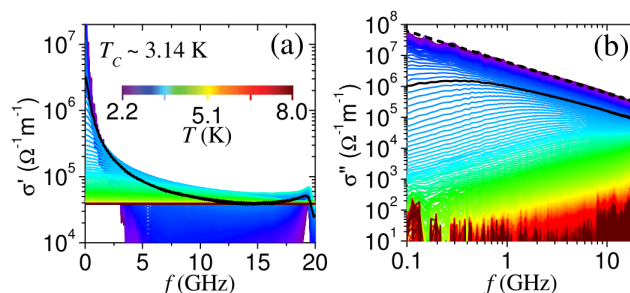


Figure 1 | ac conductivity of NbN film with $T_c \sim 3.14$ K. (a) σ' and (b) σ'' at different temperatures as a function of frequency; the solid black line shows the data at $T = T_c$. The color scale corresponding to the temperatures is shown in panel (a). The dashed line in (b) is a fit to $\sigma''(\omega) \propto 1/\omega$ for the data at 2.2 K.

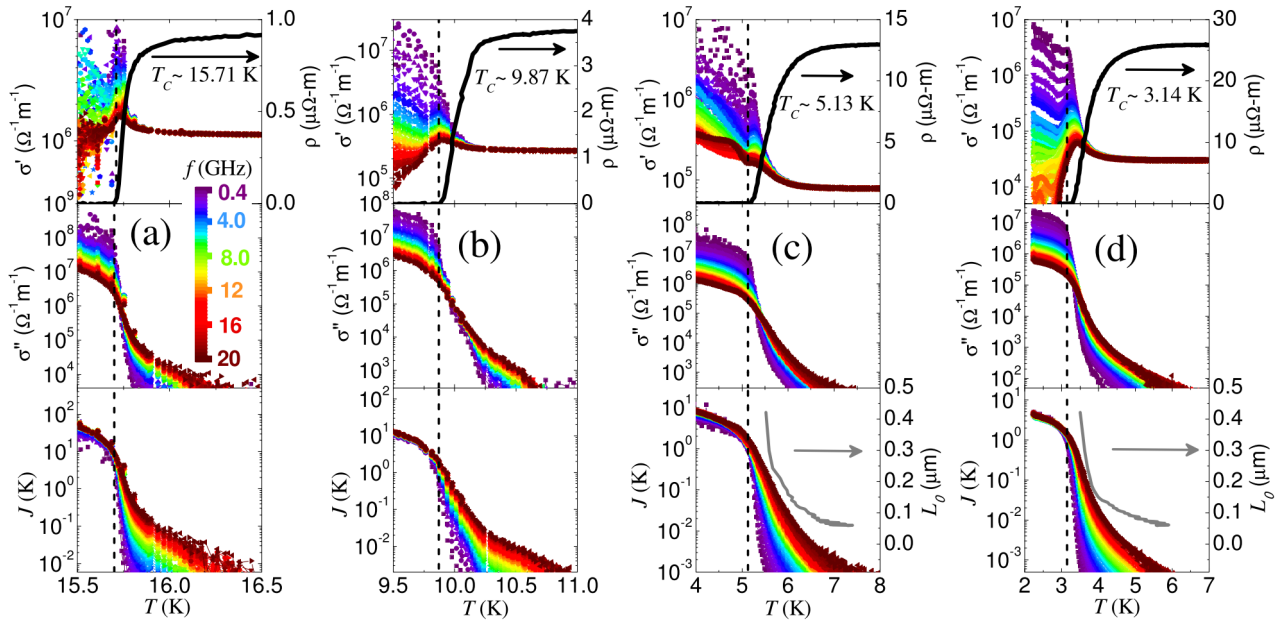


Figure 2 | Temperature dependence of σ and J at different frequencies. Temperature dependence of σ' (upper panel), σ'' (middle panel) and J (lower panel) at different frequencies for four samples with (a) $T_c \sim 15.71$ K (b) $T_c \sim 9.87$ K (c) $T_c \sim 5.13$ K and (d) $T_c \sim 3.14$ K. The color scale showing different frequencies is displayed in (a). The solid (black) lines in the top panels show the temperature variation of resistivity (ρ). Vertical dashed lines correspond to T_c . The solid (gray) lines in the bottom panels of (c) and (d) show the variation of L_0 above T_c .

very good agreement between the temperature variation of $\sigma_{fl}(0)$ and dc fluctuation conductivity, σ_{fl}^{dc} obtained from the temperature dependence of d.c. resistivity (ρ) measured in the same run (Fig. 4(c) and 4(d)) showing the consistency of our scaling procedure. We can then have a closer look at the form of the scaling function S obtained for our films. In general, the function S is constrained by the physics of the low and high frequency limits: For $\omega \rightarrow 0$, $S \rightarrow 1$ corresponding to the normal state conductivity, and for $\omega \rightarrow \infty$, $S \rightarrow c(\omega/\omega_0)^{(d-2)/z-1}$ where c is a complex constant, d is the dimension and z is the dynamical exponent, with $z = 2$ for

models based on relaxational dynamics. This is the case for ordinary GL Cooper-pairs fluctuations^{17,18}, where Aslamazov-Larkin (AL) and Maki-Thompson (MT) contributions are between the possible candidates for the observed fluctuation conductivity. Indeed, a direct comparison with the data for the sample with $T_c \sim 15.71$ K (Fig. 4(a)) shows that S matches very well with the AL prediction for $d = 2$, while MT corrections are suppressed by disorder (see Supplementary information). Observe that the 2d character of fluctuations is not surprising²⁴: Indeed even though our films are thick as compared to the zero-temperature

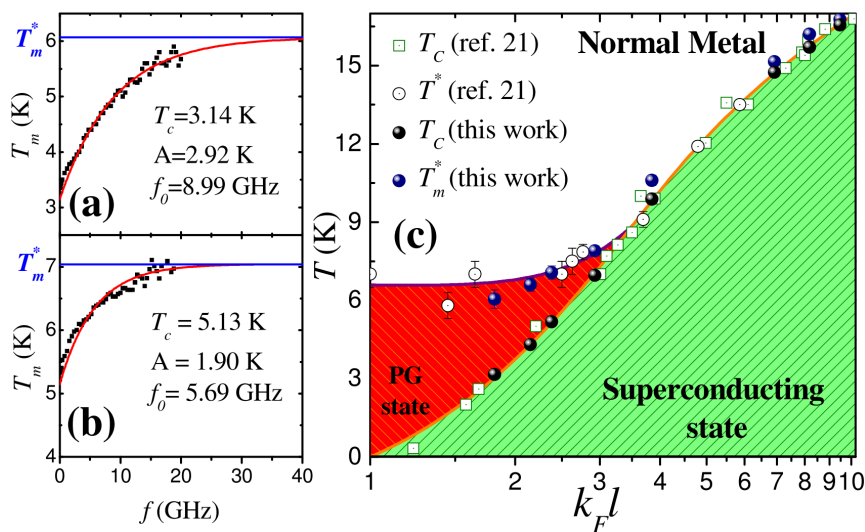


Figure 3 | Phase diagram as a function of disorder from microwave and STS measurements. (a)–(b) Variation of T_m^* as a function of frequency, f , for the sample with $T_c \sim 3.14$ K and $T_c \sim 5.13$ K respectively. The red line shows a fit of the data with the empirical relation $(T_m(f) - T_c) = A(1 - e^{-f/f_0})$; the best fit values of A and f_0 are shown in the panels. The blue lines show $T_m^* = T_m(f \rightarrow \infty)$. (c) Phase diagram showing T_c and T^* obtained from STS measurements [Ref. 21] as a function of $k_F l$ along with T_c and T_m^* obtained from microwave measurements. Samples with $T_c < 6$ K show a PG state above T_c .

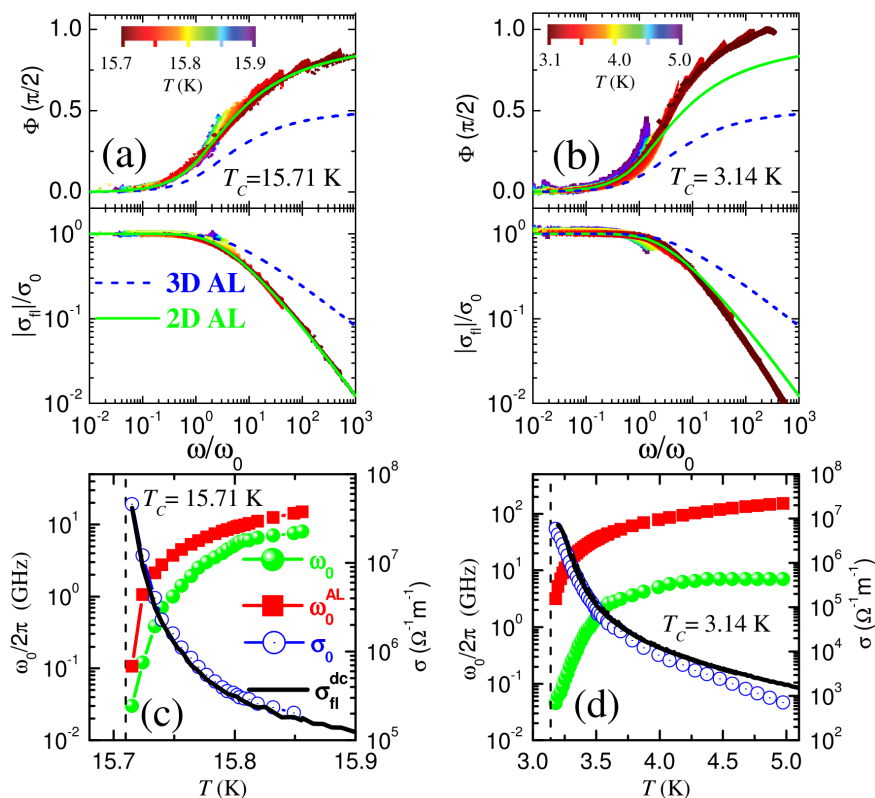


Figure 4 | Characteristic fluctuation frequency obtained from analysis of fluctuation conductivity. (a)–(b) Rescaled phase (upper panel) and amplitude (lower panel) of $\sigma_{fl}(\omega)$ using the dynamic scaling analysis on two films with $T_c \sim 15.7$ and 3.14 K respectively. The solid and dashed lines show the predictions from 2D and 3D AL theory respectively. The color coded temperature scale for the scaled curves is shown in each panel. (c)–(d) Variation of ω_0 , ω_0^{AL} , σ_0 and σ_{fl}^{dc} as a function of temperature. The dashed vertical lines correspond to T_c .

coherence length²⁰ ξ_0 , i.e. $\xi_0 < t$, in the scaling regime the T -dependent GL correlation length $\xi(T) \gg t$ is much larger than the film thickness, and GL fluctuations are effectively two-dimensional¹⁷ (see Supplementary information). On the other hand, the corresponding curve of S obtained for the sample with $T_c \sim 3.14$ K does not match at all with GL prediction, as it is better evidenced by a direct comparison between ω_0 (Fig. 4(c) and 4(d)) and the expected value from 2D AL theory, i.e. $\omega_0^{AL} = \frac{16k_B T_c}{\pi\hbar} \ln\left(\frac{T}{T_c}\right)$. Whereas for both samples $\omega_0 \rightarrow 0$ as $T \rightarrow T_c$, showing the expected critical slowing of fluctuations as the SC transition is approached, for the film with $T_c \sim 15.71$ K the best scaling value of ω_0 is in agreement with ω_0^{AL} within a factor of the order of unity, while in the film with $T_c \sim 3.14$ K ω_0 is more than one order of magnitude smaller than ω_0^{AL} . This effect cannot be attributed to a wrong choice of the scaling prefactor σ_0 , since this one still agrees very well with the measured dc fluctuation conductivity, see Fig. 4d. Instead, the lowering of ω_0 with respect to ω_0^{AL} reflects the change of the form of the scaling function S , evidenced in Fig. 4b. Moreover ω_0 remains relatively small up to temperatures as large as T^* , explaining why in the same range of probing frequencies the stiffness has a stronger frequency dependence in the sample with lower T_c . The emergence of such a low characteristic fluctuation frequency already below T^* in the most disordered sample thus signals a fundamental breakdown of the standard Cooper-pairs fluctuation scenario, which cannot be accounted for by any simple adjustment of parameters within GL theory. We note that also recent developments aimed to account for the effect of the pseudogap on the Gaussian fluctuations cannot explain our results²⁵. Indeed, the main result of Ref. [25] is that the pseudogap opening would lead to a faster suppression above T_c of the Gaussian fluctuations

with respect to the ordinary GL case, while our experimental results show a robust persistence of the fluctuation conductivity in a wide range of temperatures above T_c .

Discussion

We can now put these observations in perspective. It has been shown from STS measurements that in the presence of strong disorder the spatial landscape of the superconductor become highly inhomogeneous, thereby forming domain-like structures, tens of nm in size, where the SC order parameter (OP) is finite and regions where the OP is completely suppressed⁸. One way to visualize the superconducting state is as a disordered network of Josephson junctions, where the domains observed in STS get coupled through Josephson coupling giving rise to the global phase coherent state. In this scenario, T_c corresponds to the temperature at which the weakest couplings are broken. Therefore, just above T_c the sample consists of large phase-coherent domains (consisting of several smaller domains) fluctuating with respect to each other. We believe that the large fluctuations at low frequency in our most disordered sample originate from fluctuations between coherent domains which gradually fragment with increasing temperature. As the temperature is increased further, the large domains progressively fragment eventually reaching the limiting size observed in STS measurements at a temperature close to T^* . In such a scenario J will depend on the length scale at which it is probed. When probed on a length scale much larger than the phase coherent domains, $J \rightarrow 0$. On the other hand, when probed at length scale of the order of the domain size J would be finite. $J(\omega)$ probes the phase stiffness over a length scale set by the diffusion of the electron over one cycle of radiation which is given by $L(\omega) = [D/(\omega/2\pi)]^{0.5}$. Here, D , is the electronic diffusion constant given by, $D \approx v_F l/d$, where v_F and l are the Fermi velocity

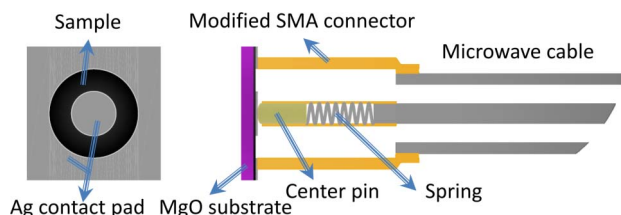


Figure 5 | Schematic drawing of the “Corbino” microwave spectrometer. Schematic drawing of the superconducting film with Ag contact pads in Corbino geometry (left) and of the 50 Ω transmission line terminating with the sample (right); a specially modified microwave connector with spring loaded centre pin is used to establish the contact with the inner and outer contact pads.

and the electronic mean free path. Therefore, for each temperature, the frequency-dependent stiffness $J(\omega)$ would vanish at a frequency such that the corresponding $L(\omega)$ becomes much larger than the size of the phase-coherent domains at the same temperature, $L_0(T)$. Using this criterion we can estimate the temperature dependence of $L_0(T) = L(\omega)$, where ω corresponds to the highest frequency which $J(\omega)$ goes below our measurement resolution at temperature T (Fig 2 (c) and 2(d)). Taking $d = 3$ in the definition of the diffusion constant (since $l < \langle t \rangle$), the limiting value of L_0 at $T \approx T^*$ is between 50–60 nm which is in the same order of magnitude as the domains observed in STS measurements⁸ on NbN films with similar T_c .

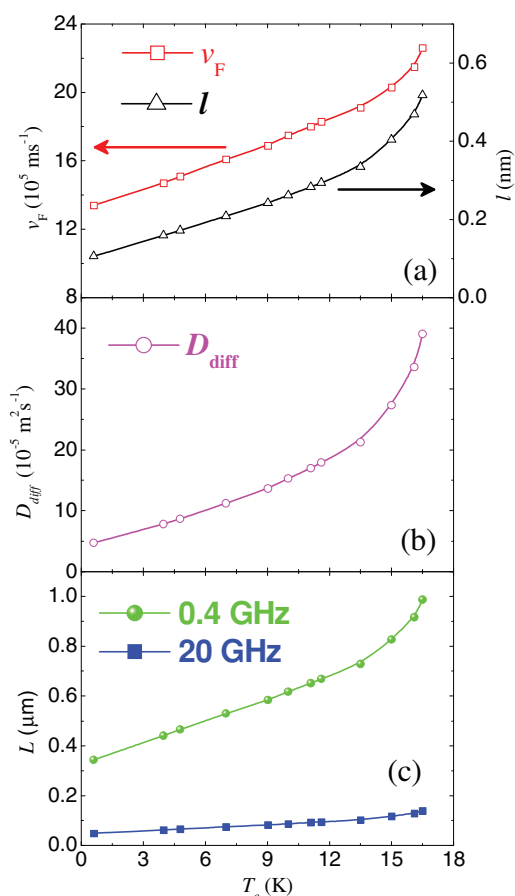


Figure 6 | Estimation of the diffusion constant for NbN thin films. (a) Variation of Fermi velocity, v_F , and electronic mean free path, l for NbN thin films with different T_c . (b) Variation of the diffusion constant, D , estimated using the values of v_F and l in panel (a). (c) Probing length scale at 0.4 GHz and 20 GHz for samples with different T_c .

In summary, we have shown that in strongly disordered NbN thin films which display a PG state, J becomes dependent on the temporal and spatial length scale for $T_c < T < T^*$. The remarkable consistency between T^* determined from STS and microwave measurements, and the evident deviations from the expected behavior for GL fluctuations, suggest the notion that the superconducting transition in these systems is driven by phase disordering of a strongly inhomogeneous superconducting background. While our results bear strong similarity with the results obtained earlier on a disordered InO_x film²⁶, we would like to note that the whole fluctuation regime cannot be attributed to Berezinskii-Kosterlitz-Thouless (BKT) physics, since earlier measurements²⁷ have shown that the BKT fluctuation regime is restricted to a narrow temperature range above T_c (see also Supplementary Material). On the other hand, the persistence far from T_c of slow relaxation processes, as characterized by the low frequency scale ω_0 , resembles the emergence of a glassy physics, which has been recently predicted at strong disorder^{12,13} and indirectly observed by STS^{6,8}. However, an explicit connection between our findings and existing predictions, as for example the relevance of a small number of percolative paths for the current at strong disorder is still lacking¹³, and its formulation would certainly improve considerably our understanding of the superconductor-insulator transition.

Methods

Sample preparation. Our samples consisted of epitaxial NbN thin films grown using reactive magnetron sputtering of Nb in Ar/N₂ gas mixture on (100) oriented single crystalline MgO substrates at 600 °C. The thickness of all samples was measured using stylus profilometer. The disorder in the form of Nb vacancies in the NbN crystalline lattice was controlled by adjusting the Nb/N₂ ratio in the plasma by controlling the Ar/N₂ ratio in the gas mixture and the sputtering power. Large Nb/N₂ ratio resulted in the non-superconducting Nb₂N crystallographic phase. At the optimal ratio we obtained stoichiometric NbN films with $T_c \sim 16$ K. Further reduction of Nb/N₂ ratio resulted in progressively disordered films with Nb vacancies with gradual suppression of T_c . These samples show remarkable consistency between T_c , ρ and $k_F l$ values. Consequently, for each sample $k_F l$ was estimated from the resistivity and T_c and ρ using the universal relation between these quantities established earlier²¹. For broadband microwave measurements, two concentric silver pads (Fig. 5) were deposited on each sample using thermal evaporation.

Measurements. $\sigma(\omega)$ was measured using a home-built broadband Corbino microwave spectrometer coupled to a continuous flow ⁴He cryostat operating down to 2.3 K. The operating frequency range of the spectrometer was 0.1–20 GHz. However, since the $\sigma(\omega)$ - T data is noisy below 0.4 GHz for the samples with high T_c (> 9 K) most of the analysis in this paper is restricted to the frequency range 0.4–20 GHz. In this technique¹⁴, concentric metallic contact pads of Ag are deposited on the superconducting films in Corbino geometry such that the inner and outer electrodes on the sample mate with the inner and outer electrode of a modified microwave connector at the end of a transmission line (Fig. 5). The sample thus acts as a terminator for an open ended transmission line. The complex reflection coefficient, S_{11} , is measured by measuring the reflected microwave signal from the sample using a vector network analyzer. Using a standard procedure²⁸, a set of three samples with well known reflection coefficient were used to correct of extraneous reflections, damping and phase shifts in the transmission line. A thick NbN film (300 nm) with $T_c \sim 16.1$ K was used as a short standard ($S_{11} = -1$) at a temperature of 2.3K. A flat Teflon piece was used for open standard ($S_{11} = 1$). A NiCr evaporated film with 20 Ω resistance between the two Corbino pads was used as a standard load. The sample impedance, Z_s , is obtained from the relation, $Z_s = Z_0(1 + S_{11}^c)/(1 - S_{11}^c)$, where S_{11}^c is the corrected reflection coefficient and $Z_0 = 50 \Omega$ is the characteristic impedance of our transmission line; $\sigma(\omega) = \frac{\ln(a/b)}{2\pi t Z_s}$ where a and b are the inner and outer diameters of the two “Corbino” electrodes. The d.c. resistance of the sample was measured in-situ using the bias-tee of the network analyzer using a two-probe technique. The temperature independent two-probe background resistance ($\sim 7 \Omega$) was subtracted while calculating the resistivity.

Determination of the electronic diffusion (D) constant and probing length of NbN films. For diffusive transport, the diffusion constant is given by, $D = v_F l/d$. Since l is much smaller than the film thickness for all our films, the electronic transport in the normal state is 3-dimensional ($d = 3$) even though the superconducting fluctuations show 2-dimensional character. To get the variation of D with disorder, we estimated v_F and l for several NbN films with T_c ranging from 16.5 K to 0.6 K. v_F and l were estimated²² from Hall coefficient (R_H) and resistivity (ρ) measured at 285 K using the free electron formulae, $v_F = \hbar(3\pi n)^{1/3}/m$ and $l = \frac{mv_F}{ne^2 \rho}$, where \hbar is the Planck’s constant, m is the electron mass and n is the carrier density given by



$n = 1/(R_{T_c}e)$. Figure 6(a) show the variation of v_{ps} l with T_c for 12 different films. The diffusion constant in the present work was estimated from T_c by interpolating the smooth variation of D vs. T_c (Fig. 6(b)). In Fig. 6(c) we plot the probing length given by $(D/f)^{1/2}$ as a function of T_c for microwave radiation with frequency of 0.4 GHz and 20 GHz.

- Bardeen, J., Cooper, L. N. & Schrieffer, J. R. Theory of superconductivity. *Phys. Rev.* **108**, 1175 (1975).
- Tinkham, M. *Introduction to Superconductivity* (Dover Publication Inc., Mineola, New York, 2004).
- Emery, V. J. & Kivelson, S. A. Importance of phase fluctuations in superconductor with small superfluid density. *Nature* **374**, 434 (1995).
- Sacépé, B. *et al.* Localization of preformed Cooper pairs in disordered superconductors. *Nature Commun.* **1**, 140 (2010).
- Mondal, M. *et al.* Phase fluctuations in a strongly disordered s-wave NbN superconductor close to the metal-insulator transition. *Phys. Rev. Lett.* **106**, 047001 (2011).
- Sacépé, B. *et al.* Localization of preformed Cooper pairs in disordered superconductors. *Nature Physics* **7**, 239 (2011).
- Sacépé, B. *et al.* Disorder-induced inhomogeneities of the superconducting state close to the superconductor-insulator transition. *Phys. Rev. Lett.* **101**, 157006 (2008).
- Lemarié, G. *et al.* Universal scaling of the order-parameter distribution in strongly disordered superconductors. (unpublished, arXiv:1208.3336).
- Ghosal, A., Randeria, M. & Trivedi, N. Role of spatial amplitude fluctuations in highly disordered s-wave superconductors. *Phys. Rev. Lett.* **81**, 3940 (1998).
- Dubi, Y., Meir, Y. & Avishai, Y. Nature of the superconductor-insulator transition in disordered superconductors. *Nature* **449**, 876 (2007).
- Bouadim, K., Loh, Y. L., Randeria, M. & Trivedi, N. Single- and two-particle energy gaps across the disorder-driven superconductor-insulator transition. *Nat. Phys.* **7**, 884 (2011).
- Feigelman, M. V., Ioffe, L. B. & Mézard, M. Superconductor-Insulator transition and energy localization. *Phys. Rev. B* **82**, 184534 (2010).
- Seibold, G., Benfatto, L., Castellani, C. & Lorenzana, J. Superfluid density and phase relaxation in superconductors with strong disorder. *Phys. Rev. Lett.* **108**, 207004 (2012).
- Kitano, H., Ohashi, T. & Maeda, A. Broadband method for precise microwave spectroscopy of superconducting thin films near the critical temperature. *Rev. Sci. Instrum.* **79**, 074701 (2008).
- Scheffler, M. & Dressel, M. Broadband microwave spectroscopy in Corbino geometry for temperatures down to 1.7 K. *Rev. Sci. Instrum.* **76**, 074702 (2005).
- Booth, J. C., Wu, D. H. & Anlage, S. M. A broadband method for the measurement of the surface impedance of thin films at microwave frequencies. *Rev. Sci. Instrum.* **65**, 2082 (1994).
- Schmidt, H. The onset of superconductivity in the time dependent Ginzburg-Landau theory. *Z. Phys.* **216**, 336 (1968).
- Aslamazov, L. G. & Varlamov, A. A. Fluctuation conductivity in intercalated superconductors. *J. Low Temp. Phys.* **38**, 223 (1980)
- Chockalingam, S. P., Chand, M., Jesudasan, J., Tripathi, V. & Raychaudhuri, P. Superconducting properties and Hall effect of epitaxial NbN thin films. *Phys. Rev. B* **77**, 214503 (2008).
- Mondal, M. *et al.* Phase Diagram and upper critical field of homogeneously disordered epitaxial 3-dimensional NbN films. *J. Supercond Nov Magn* **24**, 341 (2011).
- Chand, M. *et al.* Phase diagram of the strongly disordered s-wave superconductor NbN close to the metal-insulator transition. *Phys. Rev. B* **85**, 014508 (2012).
- Chand, M. *Ph.D. Thesis*, Tata Institute of Fundamental Research, Mumbai, India (available at <http://www.tifr.res.in/~superconductivity/pdfs/madhavi.pdf>).
- Fisher, D. S., Fisher, M. P. A. & Huse, D. A. Thermal fluctuations, quenched disorder, phase transitions, and transport in type-II superconductors. *Phys. Rev. B* **43**, 130 (1991).
- Ohashi, T., Kitano, H., Maeda, A., Akaike, H. & Fujimaki, A. Dynamic fluctuations in the superconductivity of NbN films from microwave conductivity measurements. *Phys. Rev. B* **73**, 174522 (2006).
- Levchenko, A., Norman, M. R. & Varlamov, A. A. Nernst effect from fluctuating pairs in the pseudogap phase of the cuprates. *Phys. Rev. B* **83**, 020506(R) (2011).
- Liu, W., Kim, M., Sambandamurthy, G. & Armitage, N. P. Dynamical study of phase fluctuations and their critical slowing down in amorphous superconducting films. *Phys. Rev. B* **84**, 024511(2011).
- Mondal, M. *et al.* Role of the vortex-core energy on the Berezinskii-Kosterlitz-Thouless transition in thin films of NbN. *Phys. Rev. Lett.* **107**, 217003 (2011).
- Stutzman, M. L., Lee, M. & Bradley, R. F. Broadband calibration of long lossy microwave transmission lines at cryogenic temperatures using nichrome films. *Rev. Sci. Instrum.* **71**, 4596 (2000).

Acknowledgement

We thank Peter Armitage for valuable suggestions regarding the experiment and analysis, and Claudio Castellani and Andrey Varlamov for useful discussions. L.B. acknowledges partial financial support by MIUR under project FIRB-RBFR1236VV.

Author contributions

M.M. designed and built the broadband microwave spectrometer and performed the experiments. M.M., P.R., L.B., A.K. and S.C.G. analyzed the data. J.J. and V.B. optimized the deposition conditions, synthesized the NbN films and measured the thickness. P.R. and L.B. wrote the manuscript. All authors contributed to the concept of the paper.

Additional information

Supplementary information accompanies this paper at <http://www.nature.com/scientificreports>

Competing financial interests: The authors declare no competing financial interests.

License: This work is licensed under a Creative Commons Attribution-NonCommercial-ShareAlike 3.0 Unported License. To view a copy of this license, visit <http://creativecommons.org/licenses/by-nc-sa/3.0/>

How to cite this article: Mondal, M. *et al.* Enhancement of the finite-frequency superfluid response in the pseudogap regime of strongly disordered superconducting films. *Sci. Rep.* **3**, 1357; DOI:10.1038/srep01357 (2013).